AJBAR Vol. 3(5), October 2024: 16-25, ISSN: 2811-2881

Arid Zone Journal of Basic and Applied Research

Faculty of Science, Borno State University
Maiduguri, Nigeria

Journal homepage: https://www.azjournalbar.com

Research Article

The Effect of Chitosan Surface Coating on the Properties of Zinc Ferrite Nanostructures by Sol-Gel Auto-Combustion Method Suitable for Biomedical Application

Rufus Ijeh[1*], Samson O. Aisida[2], Fabian I. Ezema[2]

[1]Department of Physics, University of Delta, Agbor, Nigeria

[2]Department of Physics and Astronomy, University of Nigeria Nsukka 410001, Nigeria

***Corresponding author's Email**: rufus.ijeh@unidel.edu.ng, doi.org/10.55639/607.02010008

ARTICLE INFO:

Keywords:
Sol-gel,
Ferrite materials,
Chitosan,
Nanostructure,
Surface coating

ABSTRACT

Zinc ferrite nanoparticles, capped with chitosan by sol-gel auto-combustion were developed in this work. The obtained nanoparticles were characterized using different techniques to confirm the physicochemical properties of the samples. The crystallinity of the samples was confirmed using X-ray diffractometer (XRD). The obtained crystallite size falls within the nanorange. Scanning electron microscopy (SEM) was used to determine the morphology of the samples. The functional groups of the samples were determined using Fourier transform infrared (FTIR) spectroscopy, and the absorbance of the sample was determined using UV-visible with Surface Plasmon Resonance (SPR) peak between 250 and 380 nm while the magnetic properties were determined using vibrating sample magnetometer (VSM). A change from paramagnetic to superparamagnetic nature was observed, making it suitable for biomedical applications. It is noteworthy that the obtained properties are highly enhanced and can be used for biomedical applications.

Corresponding author: Rufus Ijeh, **Email** rufus.ijeh@unidel.edu.ng
University of Delta, Agbor, Nigeria

INTRODUCTION

Nanomaterials have witnessed tremendous drive among researchers in our contemporary world for technological growth. This drive is due to some properties such as their surface and quantum size effects. Holistic approaches toward research into nanomaterials are potent in handling challenges aimed at diminishing sustainable development (Assey & Malasi, 2021; Sivakumara *et al.*, 2018). Nanomaterials

can be deposited using several techniques and are also affected by deposition parameters. The magnetic nanoparticles could sometimes be coated with non-magnetic material to prevent agglomeration which in turn reduces the dipole-dipole interactions and elicits biocompatibility (Zviagin *et al.,* 2016). Magnetic nanoparticles often enhance the movement of particles in the system by regulating the magnetic field. Apart from the synthesis protocol and spatial distribution of cations, factors such as the size and shape of the formulated NPs also influence the magnetic properties (Kirkpatrick *et al.,* 2023; Schiess *et al.,* 1996). Spinel ferrites have a general formula of AB_2O_4, having A and B as metal ions in their tetrahedral and octahedral sites. Among the spinel ferrites, $ZnFe_2O_4$ displays a cubic crystal structure and has numerous applications (Chavan *et al.,* 2010).

Spinel ferrites such as $ZnFe_2O_4$**,** $CoFe_2O_4$, $NiFe_2O_4$, $CuFe_2O_4$ and $MgFe_2O_4$ exhibit fascinating magnetic and electric properties which put them as important materials for commercial viability. Among the Spinel ferrites, Zinc ferrite oxide ($ZnFe_2O_4$) $ZnFe_2O_4$ is a unique material as it exhibits dual properties of ferromagnetic and semiconductor (Ebirahmi, Shahraki, & Ebirahimi). It has attracted unique attention as it is both anodic and catalytic material with proven chemical stability and for water purification (Aisida *et al.,* 2021; Aisida *et al.*, 2020b).

$ZnFe_2O_4$ has an energy band gap in the range of 2.02 eV and 2.33 eV within the UV-visible absorption spectrum, it has excellent superparamagnetic (SPION) behavior, as well as thermal conductivity for diverse application (Mataji *et al.,* 2018; Aisida *et al.,* 2023; Nakashima *et al.,* 2005) such as photocatalysis, gas sensors, Li-ion batteries and hyperthermia (Kaman *et al.,* 2024; Zhu *et al.,* 2022).

Zinc ferrite nanocrystals have been synthesized using different methods such the microemulsion method (Brown-Louisa & Hope-Weeks, 2009). Sol-gel autocombustion (Abbas, John, & Fraih, 2017), microwave-assisted (Jumeri *et al.,* 2014), chemical co-precipitation (Andhare *et al.,* 2020), Thermal (Naseri, *et al.,* 2011) and green synthesis (Jogi *et al.,* 2022). Among these methods, sol-gel auto-combustion has been ingenious for the synthesis of ferrite materials. Hence, the emplaced work used the sol-gel auto-combustion method. This method, which is a combination of sol-gel and combustion and also known as auto-ignition or low-temperature self-combustion. The method is preferred among other deposition techniques because of its good chemical homogeneity, simplicity, cost-effectiveness, control of stoichiometry, easy introduction of dopants into the final product, good crystallinity, low processing time, and ability to effectively operate at low temperatures (Gharagozlou & Bayati, 2015; Kershi *et al.,* 2023). In the sol-gel auto-combustion method, reagents can be mixed at the molecular level with good control of the accumulation of nanoparticles. It is fast and requires simple equipment for the production of high-quality homogeneous nanoparticles at large scale (Baykal *et al.,* 2014).

Biomedical applications of zinc ferrite materials have been well explored in recent years (Feng, *et al.,* 2015 ; Shapiro *et al.,* 2015). The diagnostic, therapeutic and theranostic applications of these materials have been in the limelight of research recently. A unique and essential semiconductor, zinc ferrite nanoparticles are thought to be among the most promising materials for myriad applications. Its large exciton binding energy, optical transparency and wide band gap energy are the causes of these applications. Additionally, its environmental friendliness makes it suitable for biomedical applications (Jothi, Gunaseelan, & Sagayaraj 2012; Bryan *et al.,* 2023; Li *et al.,* 2024).

Chitosan (CS) is a natural polymer that is easily decomposable by enzymes and undergoes adsorption by tissues due to its low toxicity. It is a good candidate for biomedical applications carriers for orthopedic tissue engineering, vaccine, drug delivery, gene and delivery (Raftery & Cryan, 2013). The novel of this work is centered on evaluating the impact of CS on the surface of $ZnFe_2O_4$NPs for possible biomedical applications (Aisida, Gospel, Alshoaibi & Okeudo, 2024). Our research described in this manuscript aimed to explore the potential of CS encapsulation of zinc ferrite to enhance the physicochemical properties of the formulated samples with controlled size and composition suitable for biomedical applications by a sol-gel method. The properties of the

formulated nanoparticles were examined using UV-visible, X-ray diffraction (XRD), scanning electron microscopy (SEM), elemental dispersive spectroscopy (EDS), Fourier transformed infrared spectroscopy (FTIR) and vibrating sample magnetometry (VSM) to determine their optical, structural, morphological, elemental, functional group and magnetic properties, respectively. Also, they were used to determine the impact of CS on the physicochemical properties of the formulated nanoparticles suitable for biomedical applications.

MATERIALS AND METHODS

Materials

Sigma-Aldrich products, USA of iron (III) nitrate hexahydrate ($FeNO_3 \cdot 6H_2O$) (99%), Zinc Nitrate ($ZnNO_3$. $6H_2O$) hexahydrate (99%) and chitosan ($C_6H_{11}NO_4$) were acquired from a commercial store. All the glassware was washed with Distilled water (DW).

Sol-gel auto-combustion of zinc ferrite nanoparticles

Ferric nitrate (0.4 M) and zinc nitrate (0.2 M) were homogenized in 100 ml of DW and stirred continuously at 500 rpm for 30 min for the thorough mixture. Subsequently, the obtained mixture was then heated at 80 °C in a heater and stirrer. Afterward, the gel was placed in a furnace at 60 °C for 24 h. The NPs obtained were turned to powder using a sterilized mortar. This is then followed by calcination at 500 °C for 3 h to enhance the samples. The obtained sample was labeled K1. To the homogeneous solution of K1 above, the solution of 1 g and 2 g of chitosan prepared in 50 ml of DW was added dropwise while stirring at 500 rpm for another 30 min. The procedures for K1 were observed to obtain K2 and K3.

Characterization

All the samples were analyzed using various characterization techniques. X-ray diffraction (XRD) was used to analyse the structural properties of the samples using a DW-XRD-2700A series X-ray diffractometer, Drawell International Technology Ltd., China covering a 10° to 100° range at ambient temperature. Absorbance and energy bandgap measurements of the materials were performed with a UV–visible diffuse reflectance spectroscopy (UV-DRS) using a UV-3600, (Shimadzu Co., Japan). To analyze the chemical bonds and functional groups in the samples, an FTIR (FTIR-1650, Perkin Elmer Co., USA) model spectrometer was used in the range of 4000–500cm^{-1}. The surface morphology was investigated using a scanning electron microscope (SEM1010 SEM instrument, JEOL, Ltd, Japan). The magnetic properties of the samples were examined at room temperature using a vibrating sample magnetometer (VSM), Quantum design, (VSM-4700, model) Versalab Lake Shore Co Ltd, USA, which applied a maximum field strength in the range of ± 5 kOe.

RESULTS AND DISCUSSIONS

UV Visible Analysis

The absorption of the obtained samples was obtained using UV–Vis analysis as presented in Fig. 1. The absorption bands ranged between 300 – 400nm. The observed color change confirmed the decomposition of chitosan in the formulated nanoparticles. The decomposition is a clear evidence that the material is suitable for biomedical applications (Aisida, Gospel, Alshoaibi, & Okeudo, 2024). The peak observed (i.e. the Surface Plasmon Resonance (SPR) peaks) of the Samples was determined as 356, 360 and 389 nm for K1, K2 and K3 respectively.

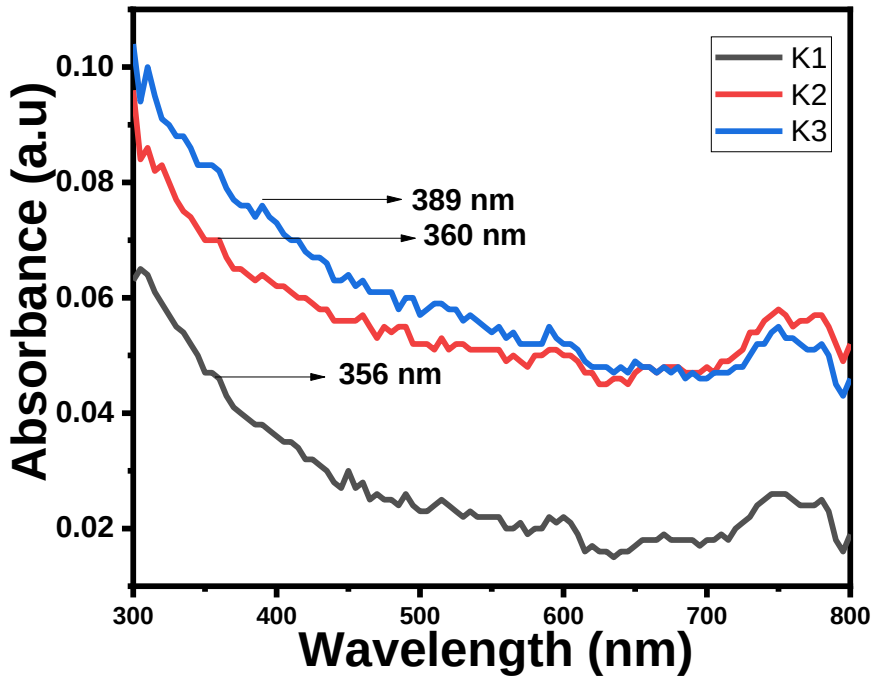

Figure 1: UV–visible analysis of samples K1, K2 and K3

FTIR analysis of the samples

The functional group inherent in CS as revealed by FTIR spectra analysis in Fig. 2, shows the main vibrations in the wavelength range of 2000 – 500 cm^{-1}. The OH functional group witnessed a blue shift from 1659 cm^{-1} for the pristine sample to 1624cm^{-1} and 1631cm^{-1} for K1 and K2 samples, respectively. The C-N functional group stretching vibration, witnessed a blue shift from 1332 cm^{-1} for the pristine sample to 1318 cm^{-1} and 1325 cm^{-1} for K1 and K2 samples, respectively. The C-O-C stretching vibration functional group also witnessed a blue shift from 1024 for the pristine sample to 1022 cm^{-1} and a red shift to 1037 cm^{-1} for K1 and K2 samples, respectively. The bands around 500 and 515 cm^{-1} are ascribed to FeO and ZnO stretching vibration bond (Aisida, Gospel, Alshoaibi, & Okeudo, 2024). This shows that the functional group really enhanced the materials for biomedical applications.

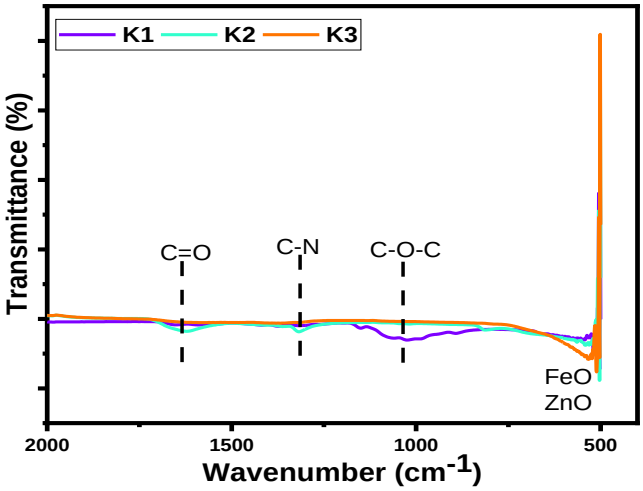

Figure 2: FTIR analysis of the samples

XRD Analysis of the samples

The XRD spectra of K1, K2 and K3 as presented in Fig. 3, shows the crystalline structure of the samples. The (311) plane exhibits the highest peaks. The major diffraction peaks observed at 2θ and the crystallographic reflection planes values are 29.86° (220), 35.18° (311), 42.66° (400), 53.02° (422), 56.62° (511) and 62.11° (440). The structure exhibited inverse spinel lattice with single-phase characteristics (Aisida, Gospel, Alshoaibi, & Okeudo, 2024). The Debye–Scherer's formula (Eq.1), was used to evaluate the crystallite size of K3 sample. The estimated value of the crystallite of 14.5 nm, falls within the nano range. The obtained crystallite size was within the range of nano-therapy and suitable for biomedical application (Aisida, Gospel, Alshoaibi, & Okeudo, 2024). The size as observed in the sample suggests that the material could exhibit good mechanical strength and stability which might be suitable for load-bearing implants or structural components requiring robustness and durability for biomedical applications (Pachamuthu, et al., 2022).

$$D_{(XRD)} = \frac{0.9\,\lambda}{\beta \cos\theta} \quad (1)$$

$D_{(XRD)}$ is the (crystalline size) expressed in (nm), λ (X-ray wavelength) (λ = 1.5406Å), β (full width at half maximum) and θ (Bragg diffraction angle) (Cullity, 1978).

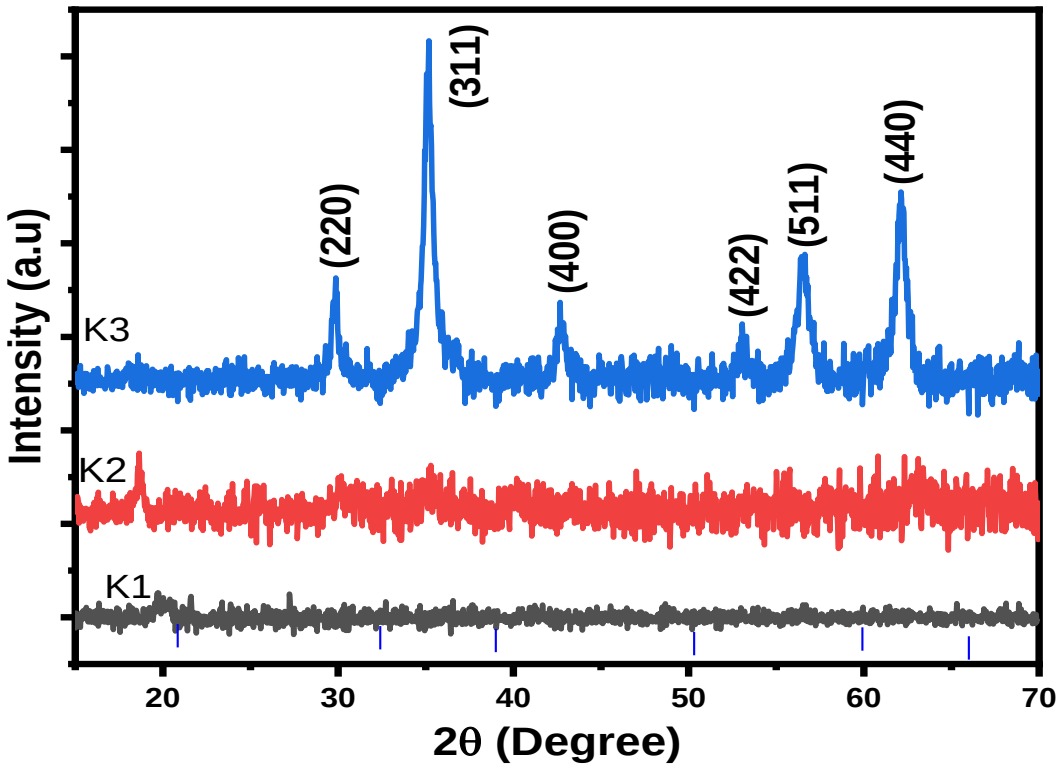

Figure 3: XRD patterns of samples K1, K2 and K3.

SEM Analysis

The SEM micrographs of K1, K2 and K3 as presented in Fig. 4, Shows spherical morphology of the samples. A spherical shape morphology was observed with Sample K1 with some aggregation. Sample K2 shows better morphologies, while K3 shows clusters of spherical morphology embedded in CS. A

similar report was also observed by Aisida *et al.* (2024). Nanospheres, nanorods, nanocapsules, nanosheet, dendrimers, nanocubes, micelles and macrophage-like shapes are all appropriate for biomedical uses (Batool *et al.,* 2023; Li *et al.,* 2024; Han *et al.,* 2022). However, the spherical-like structures are more suitable for biological uses to enhance easy flow in the blood vessels**.**

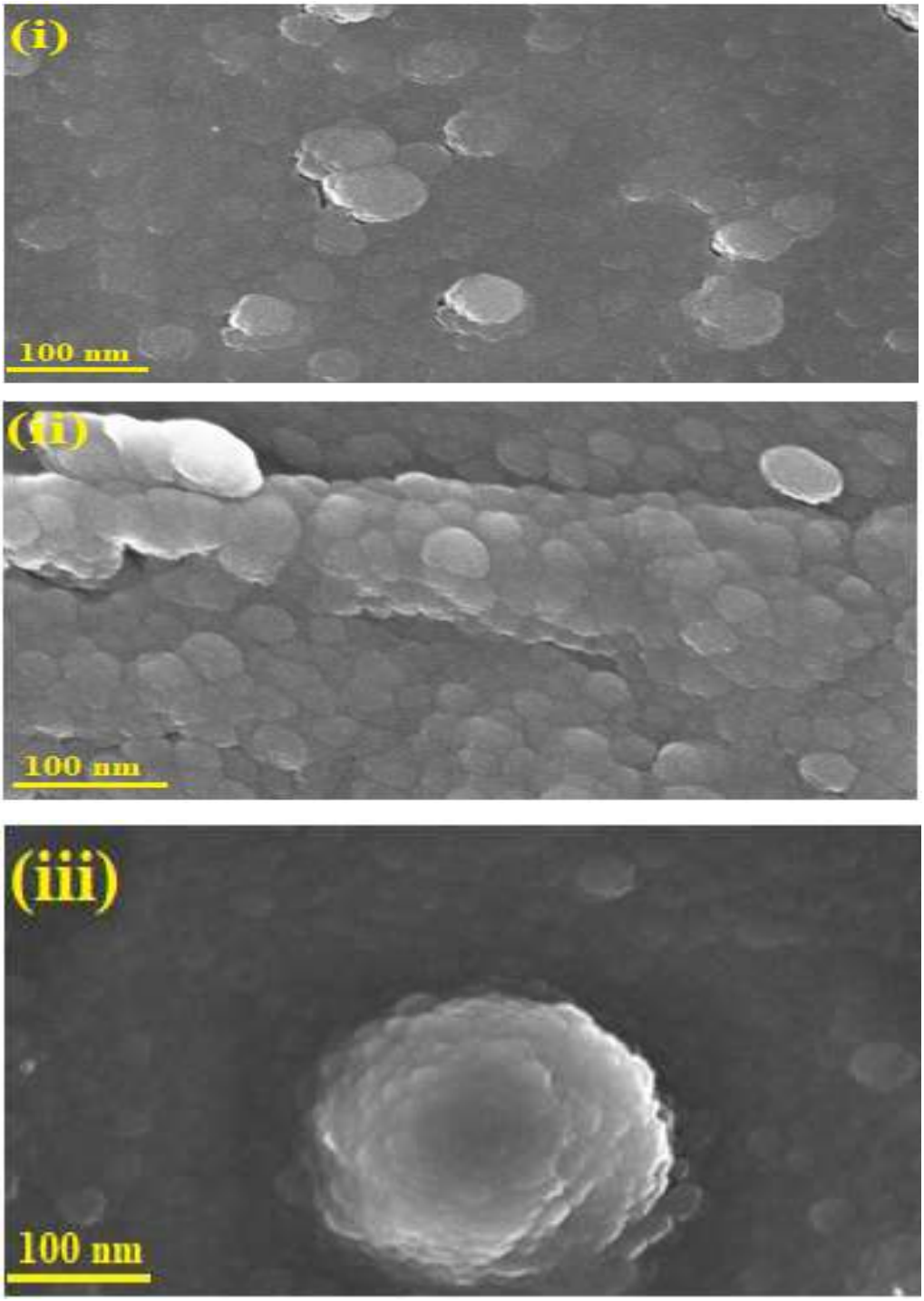

Figure 4: SEM analysis of the sample (i) K1, (ii) K2 and (iii) K3

VSM Analysis of the Samples

The magnetization against the magnetic field shows the magnetic properties of the obtained samples as shown in Fig. 5, in the range of ± 5 KOe. Table 1 shows the magnetic properties of the formulated samples. A transition from paramagnetism to superparamagnetism was observed in the samples. We deduced that the transformation is due to the doping agent. As the dopant increases, the saturation magnetization (Ms) also increases, the observed increase is as a result of the introduction of CS in the sample. This is in agreement with the previous study reported with an increase in the Ms (Ijeh *et al.*, 2019; Ijeh *et al.*, 2022b). A material with very low coercivity and remanence magnetization, but high saturation magnetization shows optimal biomedical applications. However, for effective biomedical uses, like administering medications, studies have shown that super-paramagnetic materials are more effective than ferromagnetic materials (Adam *et al.*, 2007).

Table 1: This shows the magnetic properties of the samples

Sample	Coercivity	M_r (Oe)	M_s (emu/g)
K1	572	0	0.002
K2	198	0	0.015
K3	0	0	0.17

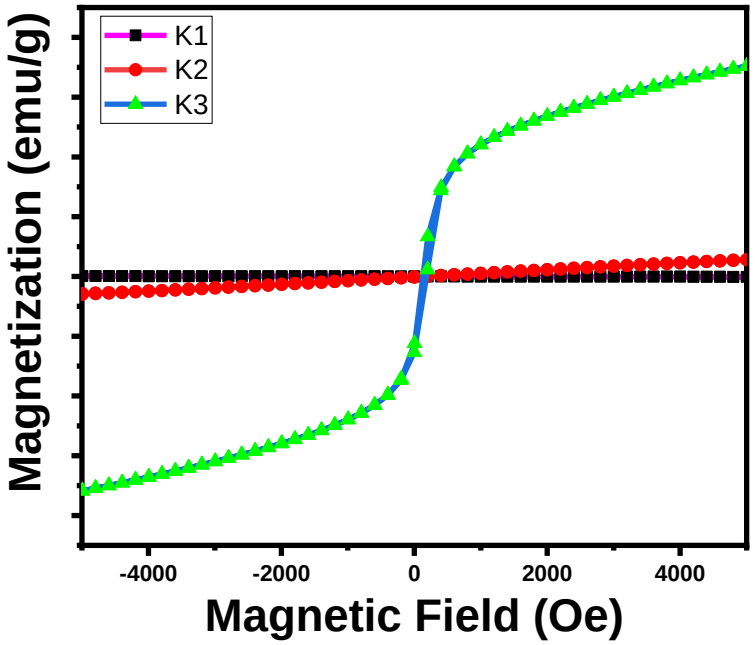

Figure 5: The magnetization against the magnetic field of the samples.

CONCLUSION

The synthesis of Zinc ferrite nanoparticles via the sol-gel auto-combustion method using Chitosan as an organic dopant has been presented in this work. The effect of chitosan on the physicochemical properties of the developed samples was investigated using various characterization techniques. The physicochemical properties of the samples were highly influenced by the introduction of CS making them more suitable for biomedical applications. A cubic crystalline spinel phase

structure of the samples was observed with the XRD, which depends on the chitosan dopant. The obtained crystallite size falls within the nanorage. A spherical morphology of the sample through SEM was observed, making it suitable for *in vivo* biomedical applications. The VSM showed a transformation from paramagnetism to superparamagnetic behavior, hence, the saturation magnetization was observed to increase with the addition of the dopant. This transformation from the paramagnetic to superparamagnetic with increase in saturation magnetization makes the materials suitable for *in vivo* biomedical applications. It is noteworthy that the obtained physicochemical properties obtained can be used for biomedical applications.

REFERENCES

Abbas, S. I., John, H., & Fraih, A. (2017). Preparation of Nano Crystalline Zinc – Ferrite as Material for Micro Waves Absorption by Sol-Gel Methods. *Indian Journal of Science and Technology, 10*(21), 1-6.

Adam, C., Janusz, S., Magda, K., & Marek, K. (2007). Hyperthermia – description of a method and a review of clinical applications. *Practical Oncology & Radiotherapy, 12*(5), 267-275.

Aisida, Ali, A., Oyewande, O. E., Ahmad, I., Ul-hamid, A., & Zhao, T. (2021). Biogenic synthesis enhanced structural, morphological, magnetic and optical properties of zinc ferrite nanoparticles for moderate hyperthermia applications. *J. Nanopart Res., 23*, 47.

Aisida, S. O., Alnasir, M. H., Botha, S., Bashir, A. K., Bucher, R., A. I., & . . . Ezema, F. I. (2020b). The role of polyethylene glycol on the microstructural, magnetic and specific absorption rate in thermoablation properties of Mn-Zn ferrite nanoparticles by sol-gel protocol. *European Polymer Journal, 109739*, 132.

Aisida, S. O., Alnasir, M. H., Botha, S., Bashir, A. K., Bucher, R., A. I., & . . . Ezema, F. I. (2020b). The role of polyethylene glycol on the microstructural, magnetic and specific absorption rate in thermoablation properties of Mn-Zn ferrite nanoparticles by sol-gel protocol. *European Polymer Journal, 132*, 109739.

Aisida, S. O., Chibueze, T. C., HAlnasir, M., Oyewande, O. E., Raji, A. T., Ekuma, C. E., . . . Ezema, F. I. (2023). Microstructural and magneto-optical properties of Co1-xNix Fe2O4 nanocomposites for hyperthermia applications. *Solid State Sciences, 136*, 107107.

Aisida, S. O., Gospel, E. C., Alshoaibi, A., & Okeudo, D. (2024). Effect of Chitosan on the Microstructural Properties of Zinc Ferrite Nanoparticles. *Macromol. Chem. Phys., 2024*, 2300375.

Andhare, D. D., Jadhav, S. A., Khedkar, M. V., Somvanshi, S., More, S. D., & Jadhav, K. M. (2020). Structural and Chemical Properties of ZnFe2O4 Nanoparticles Synthesised by Chemical Co-Precipitation Technique. *Journal of Physics: Conference Series*, 16440.

Assey, G. E., & Malasi, W. (2021). Advances in Nanomaterials Sciences and Nanotechnology for Sustainable Development:. *A Review Tanzania Journal of Science, 47*(4), 1450-1463.

Batool, A., Aisida, S. O., Javed, R., mushtaq, M., Ugwuoke, C. O., Ali, J. S., . . . Ezema, F. I. (2023). PEG Capped NixCo1−xFe2O4 Nanocomposites: Microstructural, Morphological, Optical, Magnetic, Antimicrobial, and Photodegradable Properties. *BioNanoScience, 13*, 1-12.

Baykal, A., Esir, S., Demir, A., & Güner, S. (2014). Magnetic and optical properties of Cu1−xZnxFe2O4 nanoparticles dispersed in a silica matrix by a sol–gel auto-combustion method. *Ceramics International, 41*(1), 231-239.

Brown-Louisa, P., & Hope-Weeks, J. (2009). The synthesis and characterization of

zinc ferrite aerogels prepared by epoxide addition. *Journal of Sol-Gel Science and Technology, 51*, 238–243.

Chavan, S. M., Babrekar, M. K., S., M. S., & Jadhav, K. (2010). Structural and optical properties of nanocrystalline Ni–Zn ferrite thin films. *Journal of Alloys and Compounds, 507*(1), 21–25.

Cullity, B. (1978). *Elements of X-ray Diffraction* (Vol. 102). (2nd, Ed.) London: Addison-Wesley.

Ebirahmi, M., Shahraki, R. R., & Ebirahimi, S. S. (n.d.). Method., & Masoudpanah S.M. (2014). Magnetic Properties of Zinc Ferrite Nanoparticles Synthesized by Coprecipitation. *Journal of Superconductivity and Novel Magnetism, 27*, 1587–1592.

Gharagozlou, M., & Bayati, R. (2015). Low temperature processing and magnetic properties of zinc ferrite nanoparticles. *Superlattices and Microstructures, 78*, 190–200.

Han, X., Zhao, C., Wang, S., Pan, Z., Jiang, Z., & Tang, X. (2022). Multifunctional TiO2/C nanosheets derived from 3D metal–organic frameworks for mild-temperature-photothermal-sonodynamic-chemodynamic therapy under photoacoustic image guidance. *J. Colloid Interface Sci., 621*, 360-373. doi:https://doi.org/10.1016/j.jcis.2022.04.077

Ijeh, R. O., Nwanya, A. C., Nkele, A. C., Madib, I., Khumalo, Z., Bashir, A., . . . Ezema, F. I. (2019). Magnetic and optical properties of electrodeposited anospherical copper doped nickel oxide thin films. *Physica E: Low-imensional system and nanostructures, 113*, 233-239.

Ijeh, R. O., Ugwuoke, C. O., Ugwu, E., Aisida, S. O., & Ezema, F. (2022b). Structural, optical and magnetic properties of Cu-doped ZrO2 films synthesized by electrodeposition method. *Ceramics International, 48*, 4686-4692.

Jogi, J., Singhal, S. K., Jangir, R., Dwivedi, A., Tanna, A., Singh, R., . . . Sagdeo, P. (2022). Investigation of the Structural and Optical Properties of Zinc Ferrite Nanoparticles Synthesized via a Green Route . *journal of electronin Materials, 51*(12), 5482-5491.

Jothi, N. N., Gunaseelan, R., & Sagayaraj, P. (2012). Investigation on the synthesis, structural and optical properties of ZnO nanorods prepared under CTAB assisted hydrothermal conditions. *Archives of Applied Science Research, 4*, 1698-1704.

Jumeri, F., Lim, H., Ariffin, S., Huang, N., Teo, P., Fatin, S., . . . Harrison, I. (2014). Microwave Synthesis of Magnetically Separable ZnFe2O4-Reduced Graphene Oxide for Waste water Treatment. *International Journal of Ceramic Engineering & Science, 40*, 7057.

Kaman, O., Kubániová, D., Kubíčková, L., Herynek, V., Veverka, P., Jirák, Z., . . . Kohout, J. (2024). Magnetic particle spectroscopy and magnetic particle imaging of zinc and cobalt ferrite ferrite nanoparticles: Distinct relaxation mechanisms. *Journal of Alloys and Compounds, 978*, 173022.

Kershi, R. M., Alshehri, A. M., & Attiyah, R. M. (2023). Enhancement of Ni–Zn ferrite nanoparticles parameters via cerium element for optoelectronic and energy applications. *Discover Nano, 18*, 1.

Kirkpatrick, K. M., Zhou, B. H., Bunting, P. C., & & Rinehart, J. D. (2023). Quantifying superparamagnetic signatures in nanoparticle magnetite: A generalized approach for physically meaningful statistics and synthesis diagnostics. *Chemical Science,, 14*(27), 7589-7594.

Li, B., Wang, W., Zhao, L., Li, M., Yan, D., Li, X., & Liao, Y. (2024). Aggregation-Induced Emission-Based Macrophage-Like Nanoparticles for Targeted Photothermal Therapy and Virus Transmission Blockage in Monkeypox. *Adv Mater., 36*, 2305378. doi:doi: 10.1002/adma.202305378.

M. Iv, N. T., Feng, D., Holdsworth, S. J., Yeom, K. W., & Daldrup-Link, H. E. (2015). Clinical applications of iron oxide nanoparticles for magnetic resonance imaging of brain tumors. *Nanomedicine , 10*, 993–1018.

Mataji, M., Ghorbani, M., & Gatabi, M. P. (2018). Structural, optical and magnetic properties of novel ZnFe2O4/ZrO2 mixed metal oxide nanocomposite synthesized by hydrothermal technique. *Journal of Alloys and Compounds*, *298-309*, 757.

Nakashima, S., Fujita, K., Tanaka, K., & & Hirao, K. (2005). High magnetization and the high-temperature superparamagnetic transition with intercluster interaction in disordered zinc ferrite thin film. *Journal of Physics Condensed Matter, 17*, 137–149.

Naseri, M., Saion, E. B., Hashim, M., Shaari, A., & Ahangar, H. (2011). Synthesis and characterization of zinc ferrite nanoparticles by a thermal treatment method. *Solid State Communications, 151*, 1031–1035.

Pachamuthu, P., Jeyakumari, A. P., Srinivasan, N., Chandrasekaran, R., Revathi, K., & Karuppannan, P. (2022). Structure, surface analysis and bioactivity of Mn doped zinc oxide nanoparticles. *Journal of the Indian Chemical Society, 99*, 100342.

Raftery, R., & Cryan, A. (2013). Chitosan for Gene Delivery and Orthopedic Tissue Engineering Applications. *Molecules*, *18*(5), 5611-5647.

Schiess, W., Potzel, W., Karzel, H., Steiner, M., Kalvius, G. M., Martin, A., . . . spinel., &. W. (1996). Magnetic properties of the ZnFe2O4. *Physical Review B, 53*, 9143.

Shapiro, B., Kulkarni, S., Nacev, A., Muro, S., Stepanov, P. Y., & Weinberg, I. N. (2015). Open challenges in magnetic drug targeting, Wiley Interdiscip. Rev.-Nanomed. . *Nanobiotechnol., 7*, 446–457.

Sivakumara, P., Thyagarajanb, K., & Kumar, A. (2018). Investigations on physical properties of Zn ferrite nanoparticles using Sol-gel auto combustion technique Digest;. *Journal of Nanomaterials and Biostructures, 13*(4), 1117-1122.

Zhu, J., Zhu, Y., Chen, Z., Wu, S., Fang, X., & Yao, Y. (2022). Progress in the Preparation and Modification of Zinc Ferrites Used for the Photocatalytic Degradation of Organic Pollutants. *International Journal of Environmental Research and Public Health,, 19*(17).

Zviagin, V., Kumar, Y., Lorite, I., Esquinazi, P., Grundmann, M., & Schmidt-Grund, R. (2016). Ellipsometric investigation of ZnFe2O4 thin films in relation to magnetic properties. *Applied Physics Letters, 108*, 131901.